journal

J. Am. Ceram. Soc., 92 [11] 2731–2737 (2009)
DOI: 10.1111/j.1551-2916.2009.03271.x

Diffusion of Water Species in Yttria-Stabilized Zirconia

Tuan Duong, Andi M. Limarga, and David R. Clarke[†,‡]

Materials Department, College of Engineering, University of California, Santa Barbara, California 93106-5050

The diffusion of moisture-related species into both tetragonal and cubic single crystals at temperatures characteristic of moisture-enhanced low-temperature degradation of tetragonal zirconia is reported using secondary ion mass spectrometry (SIMS). The crystals were immersed in D and O^{18} isotopically labeled water and in O^{18} gas environments over the temperature range of 100°–220°C and SIMS profiles of H, D, O^{18}, and $O^{18}D$ determined. The oxygen diffusivities in both tetragonal and cubic crystals were the same, irrespective of whether the crystals were exposed to gas or water. Furthermore, the oxygen diffusivities were consistent with extrapolations of the oxygen diffusivities in cubic crystals reported at higher temperatures using the reported activation energy for oxygen vacancy diffusion. Both H and D diffuse into the tetragonal crystal when immersed in water but despite having a higher concentration of vacancies no diffusion of H or D was detectable in the cubic single crystals exposed under identical conditions. Quantification of the H and D diffusion into the tetragonal crystal proved unreliable due to charging effects even though the SIMS profiling was performed at liquid nitrogen temperatures. Nevertheless, it was concluded that D can diffuse in tetragonal zirconia at room temperatures over a period of several months. Finally, although a species of mass 20 amu, which is the same as the isotopic labeled OH ($O^{18}D$) ion, was detected in the tetragonal single crystal zirconia exposed to water, it was concluded that this was a SIMS artifact and that moisture does not diffuse in zirconia as either an OH or H_2O ion.

I. Introduction

As early as 1981 it was discovered that yttria-stabilized zirconia ceramics would slowly transform from the tetragonal to its monoclinic form in the presence of moisture[1] at temperatures as low as room temperature. This phenomenon, commonly referred to as low-temperature degradation (LTD) on account of the reduction in strength of the ceramic accompanying the transformation, occurs at a rate that depends on temperature, the humidity, and the concentration of the yttria stabilizer.[2–4] It is of importance because the transformation occurs over a temperature range, typically room temperature to 100°–400°C, over which zirconia has found several important applications such as biomedical implants[3] and coatings.[5] It is also significant because the moisture-enhanced transformation competes with crack propagation-induced transformation, as in transformation toughening, as a process by which metastable tetragonal converts to the stable monoclinic polymorph.

A variety of qualitative explanations associated with the inward diffusion of moisture species have been proposed to account for the kinetics of the transformation. Most invoke the idea that OH^- ions diffuse into the zirconia lattice, filling oxygen vacancies, and reducing the stabilization of the tetragonal phase. In support of this is the reported similarity between the apparent activation energy of the transformation kinetics and the activation energy for oxygen vacancy diffusivity.[6,7] The latter have been measured in cubic single crystals at higher temperatures (above ~500°) than the lower temperatures at which LTD occurs. A number of species on the surface of zirconia exposed to water have been identified by X-ray photoelectron spectroscopy.[8] These include OH^- and O_2^- ions. In addition, there is one report by elastic recoil analysis indicating the presence of hydrogen in zirconia samples exposed to water at 200°C in an autoclave.[9] Lastly, there are a number of papers in which an infrared absorption band characteristic of the presence of OH^- has been reported in zirconia ceramics after exposure to water using infrared spectroscopy but again no quantitative information concerning diffusivities has been obtained.

In the absence of quantitative data and equivocal species identification, we describe a number of diffusion experiments, using ^{18}O and D isotopically labeled water, to determine the nature of moisture diffusion in zirconia. These isotopes were chosen so that it would be possible to monitor a variety of moisture-derived species, including H, O, OH, and H_2O. Measurements were made on both single crystals of tetragonal and cubic yttria-stabilized zirconia using secondary ion mass spectrometry (SIMS). Although, as will be seen, SIMS analysis of H and D is not ideal because of the sensitivity to surface charging induced effects, the technique nevertheless provides information on the diffusing species and quantitative information regarding their diffusivities.

II. Experimental Procedure

All the samples for the diffusion experiments were either cut from a large boule of a tetragonal single crystal of nominal composition 3 m/o Y_2O_3 (6 m/o $YO_{1.5}$), made by skull melting (Ceres Corporation, Niagara Falls, NY), or were cut from commercially available cubic single crystals stabilized with 9 m/o Y_2O_3 (Zirmat Inc., North Billerica, MA). The actual composition of the boule was found to be 6.17 ± 0.13 m/o $YO_{1.5}$ using electron microprobe microanalysis determined from an average of 23 locations. The tetragonal boule was oriented using X-ray diffraction and slices cut parallel to (001). Samples, approximately 5 mm × 3 mm × 2 mm, were cut from the slices using a slow speed diamond saw and mechanically wet polished using diamond lapping films from 9 to 1 μm. It was found that there was no difference in the isotopic diffusion profiles between samples that had been cut and polished in oil or water. After polishing, all the tetragonal samples were cleaned in an ultrasonic bath with acetone and isopropanol alcohol. A number of the cubic single crystals, believed to have been Siton polished by the supplier, were annealed in air at 1200°C for 2 h rather than being mechanically polished.

For the diffusion experiments, individual samples were loaded into separate stainless-steel Swagelok tubes fittings containing 0.3 mL of an equal mixture of deionized water and deuterated water with ^{18}O, $D_2^{18}O$. In accord with the manufacturer's instructions, the tube caps were turned finger tight and then additionally turned a quarter rotation with a wrench. A K-type thermocouple was attached to the tube fitting and then

I.-W. Chen—contributing editor

Manuscript No. 25981. Received March 8, 2009; approved June 8, 2009.

This work was supported by the National Science Foundation through the DYNES program, grant number DMR-0605700.

[†]Author to whom correspondence should be addressed. e-mail: clarke@seas.harvard.edu

[‡]Present address: School of Engineering and Applied Sciences, Harvard University, Cambridge, MA 02138

the tubes inserted into a tube furnace. Each diffusion experiment was performed as follows: (1) a 30-min heating to the desired diffusion temperature, (2) an isothermal soak period, and (3) a 15-min cooling period to room temperature. A range of diffusion temperatures, from 100° to 200°C, as well as diffusion times were investigated. After the diffusion anneal and cooling, the samples were removed and cleaned in an ultrasonic bath with acetone and isopropanol alcohol to remove surface water before inserting into the vacuum system of the SIMS system.

Diffusion profiles for each sample were obtained using dynamic SIMS (Physical Electronics 6650 Quadrupole system, Eden Prairie, MN). Samples were first cooled in the analytical chamber using liquid nitrogen and analysis was carried out in a vacuum of $\sim 5 \times 10^{-10}$ torr. The SIMS profiling was performed with the sample cooled to liquid nitrogen temperature to minimize any possibility of diffusion of the H and D under the ion beam. A 6 kV Cs^+ ion beam was used with the quadruple detector set to collect secondary negative ions. Concurrently, surface charge compensation was supplied by an electron gun. Secondary ion counts of hydrogen and oxygen isotopes (H, D, and ^{18}O) as well as other species $D^{18}O$ (mass 20) were recorded under the control of the SIMetric software as a function of analysis time. In the particular SIMS machine used, the detector system nonlinearity leads to the center of mass for H and D, being at 1.2 and 2.1 amu, respectively. A channel width of 0.2 amu was used for the collection of all the species, except for the H and D, where a wider channel (0.3 amu) was used. In addition, the counts at 18.4 amu were used to monitor the ^{18}O concentration as the 18 amu signal was so strong that it often saturated the collector. Depth profiles of the SIMS crater was measured after SIMS analysis using a Sloan Dektak IIA profilometer (Veeco, Santa Barbara, CA) to calibrate the analysis time to a corresponding depth with the assumption of a constant ion erosion rate.

To complement the aqueous diffusion studies, a number of gaseous diffusion studies were also carried out in which the tetragonal and cubic crystals were annealed in O^{18} gas at two different temperatures. These experiments were designed to provide oxygen diffusion data at significantly lower temperatures than hitherto reported, commensurate with the moisture diffusion studies. They were carried out in a special apparatus, similar to that described in reference Manning *et al.*,[10] in which the crystals were annealed in one atmosphere of a 1:4 mixture of 99% pure O^{18}: argon gas (America Speciality Gases, Toledo, OH). The crystals were placed in silica tubes, the air evacuated and then replaced with the O^{18} gas mixture and annealed in a tube furnace. After gaseous annealing, the crystals were removed and the concentration profile of O^{18} was determined by SIMS in the same manner as described for the samples exposed to water.

The surfaces of the crystals before and after water exposures were monitored by optical microscopy and by Raman microscopy. The latter was carried out using a confocal Raman microscope system (LabARAMIS system, Jobin-Yvon, Edison, NJ) and with excitation at 633 nm from a HeNe laser.

To calibrate the SIMS sensitivity for both H and D in zirconia, a cubic single crystal was co-implanted with a H dose of 1.2×10^{14} cm^{-2} and a D dose of 1.7×10^{14} cm^{-2} at energies of 33 keV each. Based on SRIM/TRIM simulations, the peak concentrations of the two ions were calculated to lie at 200–400 nm below the surface with a peak width of 50–100 nm.

III. Results

The SIMS profile recorded from the H and D implanted calibration crystal is reproduced in Fig. 1. The peak in the D concentration is at 400 nm, the expected range based on SRIM simulations. The implanted H also exhibits a range of implantation concentration but its' peak occurs, in agreement with the simulations, at a smaller depth. An unexpected feature of the

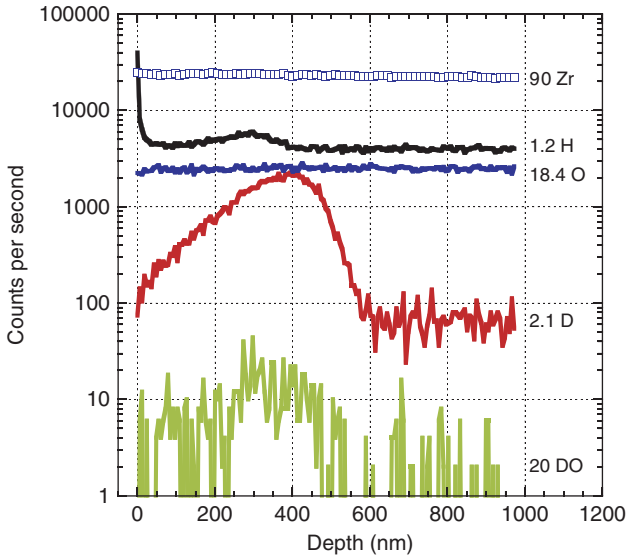

Fig. 1. Secondary ion mass spectrometry (SIMS) profiles of a cubic zirconia single crystal after implantation of 1.2×10^{14} atoms/cm^2 H ions and 1.7×10^{14} atoms/cm^2 D ions. In this and subsequent figures, the SIMS profiling was performed using a 6 kV Cs^+ ion beam.

profiles, however, is the appearance of a weak but quite distinct profile in the mass 20 amu concentration having a similar profile to that of the D profile. This is a remarkable finding because mass 20 is not an ion that is present in the crystal and can only be obtained from the implanted D with an ion of mass 18 amu, or most unlikely, a combination of two D ions and one ^{16}O ion, namely $D_2^{16}O$. As ^{18}O was not implanted into the crystal its only possible source is as the naturally occurring oxygen isotope in the crystal. (The natural isotopic abundance of ^{18}O is 0.02%.) Either way, the observation of mass 20 amu, which has the same mass as $D^{18}O$, has important implications in the context of the results reported later in this section.

Figure 2 shows an example of the near surface O^{18} ion diffusion profiles in a tetragonal crystal, measured after exposure for the same duration at different temperatures in the isotopically enriched water, in terms of the collected counts per second as a function of depth. Similar profiles were recorded for ions with mass 20 amu ($D^{18}O$) but are not plotted here. (The species H_2O has a mass of 18 amu and hence is indistinguishable from O^{18}.) No ions with a mass number of 22, corresponding to water molecules, D_2O^{18}, were detectable. The concentration profiles of the O^{18} in the tetragonal crystals, as well as the mass 20 amu

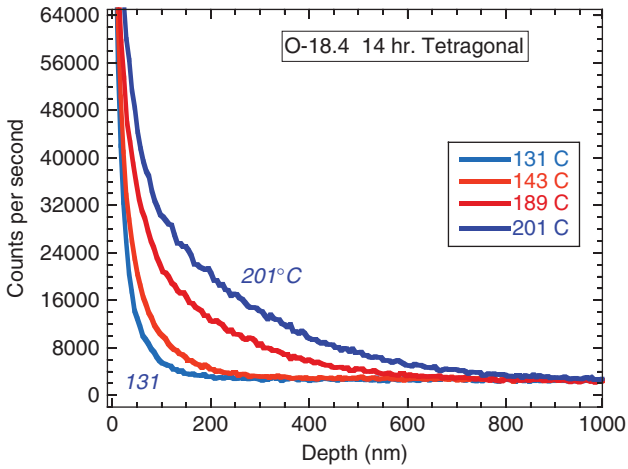

Fig. 2. Near surface secondary ion mass spectrometry profiles of ^{18}O in tetragonal zirconia after exposure to the isotopically enriched water for 14 h at the temperatures indicated. Similar profiles, not shown, were also obtained for mass 20 amu.

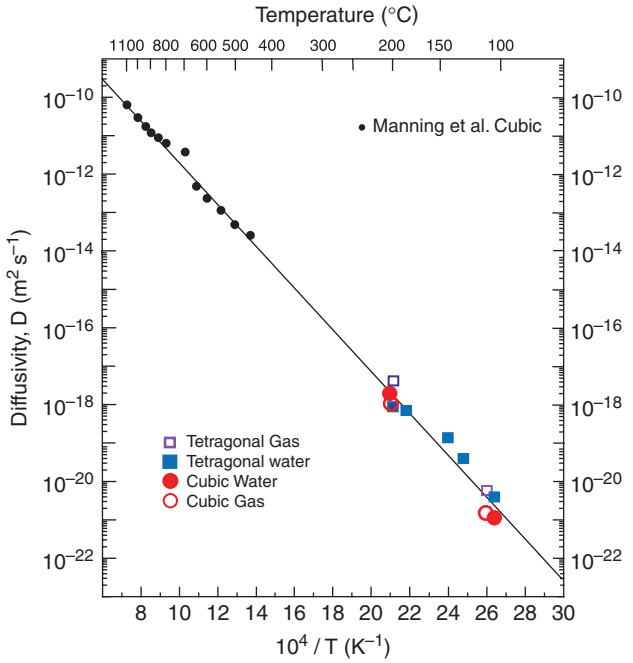

Fig. 3. Summary of the oxygen diffusivity results from the different diffusion experiments superimposed on an Arrhenius plot with the results for oxygen diffusion at high temperatures from reference Manning *et al.*[7]

concentration profiles, could be fit by the standard one-dimensional equation for inward diffusion from a constant planar surface source:

$$\frac{c(x,t) - C_S}{C_0 - C_S} = \text{erf}\frac{x}{2\sqrt{(D,t)}} \quad (1)$$

where C_S and C_0 are the surface concentration and initial, back ground concentrations, respectively, x is the distance into the material, t is the diffusion time, D is the diffusivity.

The diffusivities obtained from the short time exposures for the O^{18} ions are shown as data points in Fig. 3 superimposed on a plot of the diffusivity of oxygen vacancies in cubic zirconia, taken from references,[6,10] and extrapolated to low temperatures. As will be described later, similar diffusivities were also recorded for the cubic single crystals and are indicated on Fig. 3. The same values for the diffusivities were obtained for the 20 amu species.

The diffusion profiles of H, D, ^{18}O, and $D^{18}O$ in the tetragonal crystals, after exposure to the isotopically enriched water all had a similar shape as illustrated in Fig. 4 for a crystal after being immersed in water for 14 h at 142°C. The profiles are unlike the standard inward diffusion profiles in having, in addition to the standard inward diffusion profile, marked A, an almost linear slope of the logarithm of counts versus depth at intermediate depths, region B, followed by a more characteristic decay deeper into the crystal, region C, until merging into a constant background level, G. Notably, the profiles of all the possible diffusing species are similar in shape with the rapid decay occurring at the same depth in the crystal for each species. By contrast, the Zr and Y profiles (the latter not shown) are constant with depth as expected. The profiles at short depths of the $^{18.4}O$ and mass 20 amu both had the expected decay profiles characteristic of inward diffusion of the species given by Eq. (1). None of the distinctive diffusion regimes was linear on a plot of log counts vs depth to the 6/5th power, characteristic of short circuit diffusion, for instance along grain boundaries or dislocations.[11,12] Unfortunately, the D and H profiles near the surface, typically within ~200 nm of the surface, were not very reproducible, varying from one SIMS analysis to another. This

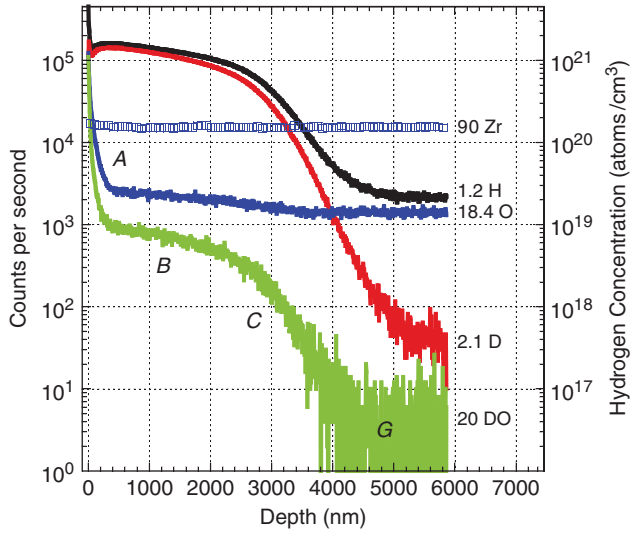

Fig. 4. Secondary ion mass spectrometry profiles for a tetragonal single crystal after exposure to isotopically enriched water for 14 h at 142°C. Three different regimes, A, B, and C, of the diffusion profiles are identified. The back ground level is labeled G. The hydrogen concentration obtained using the relative sensitivity factor in the Appendix A is plotted on the right hand axis.

variability was attributed to the sensitivity of the H and D signals to the establishment of the charge neutrality conditions in the SIMS. For this reason, the initial portions of the D and H profiles were ignored and only the deeper portions of the profiles taken into account. As will be described later, Raman spectra recorded from the crystals indicated that the crystal surface was partially transformed to monoclinic after exposure to the isotopically enriched water.

A similar deuterium profile as shown in Fig. 4 after immersion and then after seven months in ambient air at room temperature and then again after short annealing is shown in Fig. 5. The comparison clearly shows that the D species has some mobility over a period of 7 months at room temperature diffusing both to the surface and, to a lesser extent, also diffusing further into the crystal. The decreased integrated intensity also indicates that there is net diffusion out of the crystal with aging. Subse-

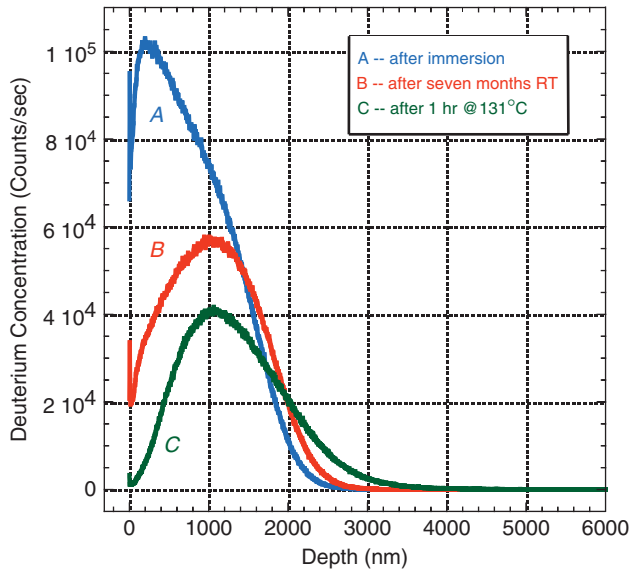

Fig. 5. The effect of aging on the D concentration after an initial exposure to deuterated water at 131°C for 36 h. (A) Immediately after immersion, (B) after 7 months in ambient air, and (C) after subsequent heating for 1 h to 131°C. After 7 months in ambient air at room temperature, the peak concentration decreases and the profile broadens indicating D diffusion at room temperature.

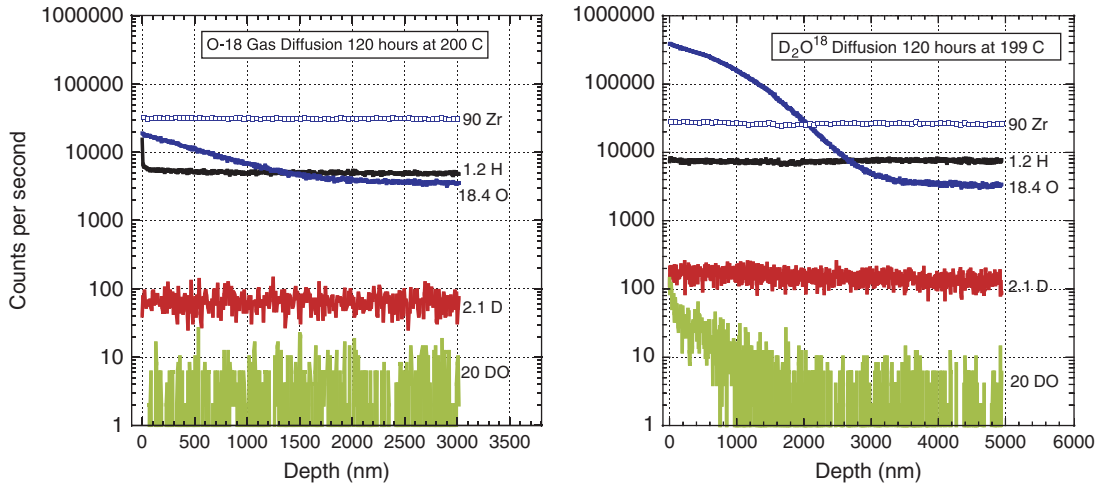

Fig. 6. Secondary ion mass spectrometry profiles for a cubic zirconia single crystal after exposure to ^{18}O gas for 120 h at 200°C (left) and after exposure to isotopically enriched water for the same time and temperature (right). The profiles demonstrate that neither H nor D diffuse into cubic yttria-stabilized zirconia. The mass 20 signal is believed to be an artifact as discussed in the text. The H and D background counts differ slightly in the two profiles on account of differences in charge compensation and collection efficiency for H and D from an insulating solid.

quent heating to 131°C for 1 h causes further redistribution with more diffusion to the surface as well as further diffusion deeper into the crystal. Significantly, the crystal remained monoclinic after annealing as determined from its Raman spectrum.

In Fig. 6, the diffusion profiles for a cubic single crystal exposed to gaseous ^{18}O for 120 h at 200°C are compared with those for another piece of the same crystal after being immersed in the isotopically enriched water for the same time and almost the same temperature (199°C). The ^{18}O diffusion profile in the crystal exposed to the gas follow the standard diffusion profile (Eq. (1)) and equally good fits, with a correlation coefficient of better than 0.999, could be obtained using either the standard one-dimensional diffusion equation or with that modified to account for surface exchange.[10] The diffusivities measured at different temperatures lie well within the range of oxygen diffusion coefficients obtained by extrapolating those reported in the literature for cubic zirconia at temperatures above 450°C to lower temperatures. The extrapolation assumes the same activation energy of 1.0 eV as has been reported for the high temperature diffusion measurements. The diffusion profile for the ^{18}O ions in the crystal exposed to the isotopically enriched water is the same as in the crystal exposed to gas although the magnitude of the counts is noticeably greater. (The back ground level is the same.) As with the SIMS calibration experiments, there is an apparent diffusion profile for mass 20 amu which we again attribute to a measurement artifact because the concentration profile follows that of the ^{18}O ions. Most significantly, though, is that there is no evidence for any inward diffusion of either D or H into the cubic crystal from the water and the D and H counts are essentially identical to those in the crystal exposed to air, namely they have similar back ground levels. (The variation in D and H counts between these two profiles, which were recorded in separate sets of SIMS measurements, is an example of the variability associated with the charge neutralization process.) The only exception we found was when mechanically polished cubic crystals were immersed in water rather than those annealed at 1200°C. Then, the D and H concentration profiles fit a 6/5th depth dependence, suggesting that they diffused along dislocations introduced into the surface by the polishing.

Figure 7 is a similar comparison to that of Fig. 6 but for pieces of the tetragonal crystal cut from the same boule. (Both the profiles in Figs. 6 and 7 were obtained from cubic and tetragonal crystals annealed together to ensure the most direct comparison.) For the tetragonal crystal exposed to water, in diffusion regime A, the ^{18}O concentration again fits the standard diffusion equation (Eq. (1)) and the diffusivity determined is the same as in the cubic crystal. Interestingly, as with the data from the cubic crystal, the mass 20 signal follows the same profile shape as does the ^{18}O concentration but as suggested by the data in Fig. 1 is likely to be a measurement artifact. The most striking

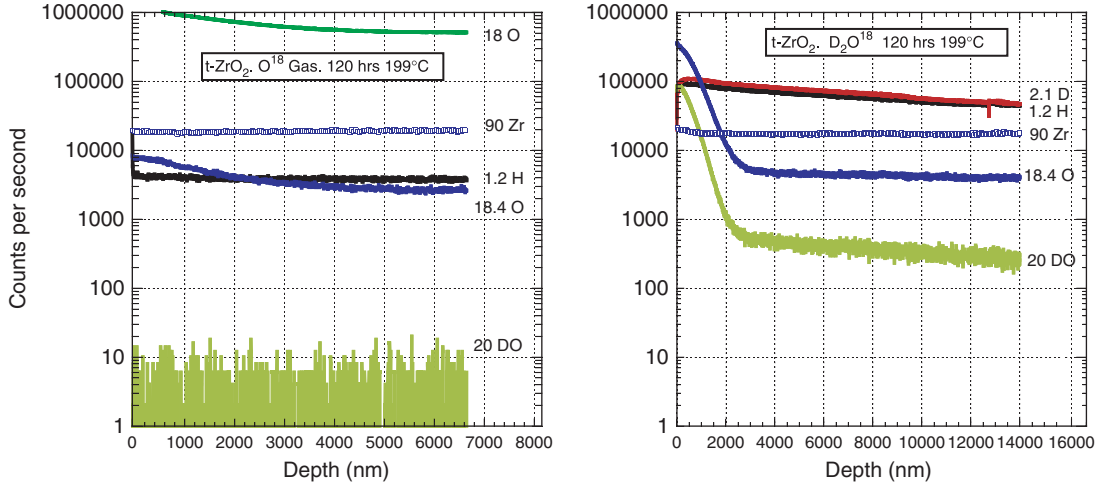

Fig. 7. Secondary ion mass spectrometry profiles for a single crystal tetragonal zirconia after exposure to ^{18}O gas for 120 h at 200°C (left) and after exposure to isotopically enriched water for the same time and temperature (right).

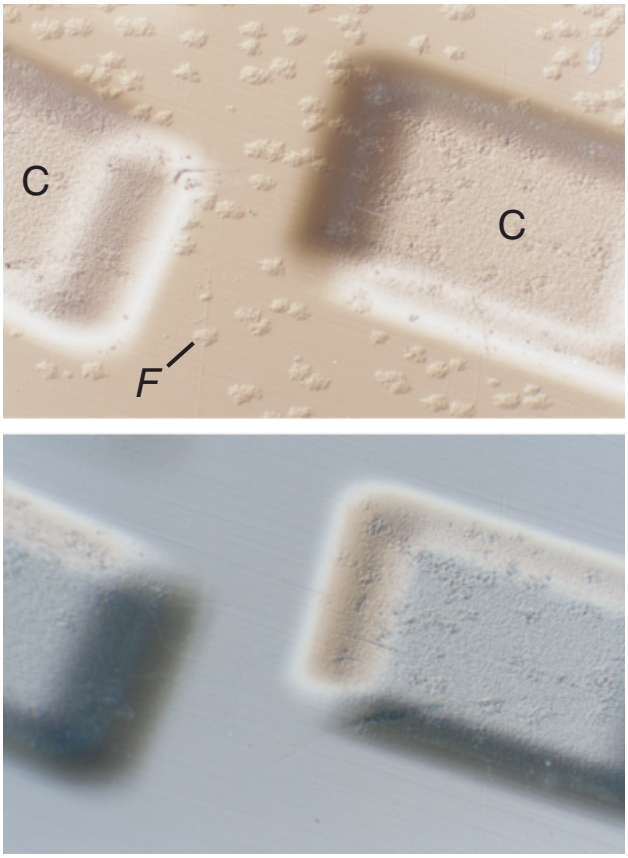

Fig. 8. Optical micrographs of the surface of a tetragonal crystal that had been polished and then immersed in water for 14 h at 122.5°C (top) and then after subsequent annealing at 1200°C for 2 h (bottom). The crystal surface before exposure was featureless but after immersion in water had an "orange peel" appearance which in the micrographs is due to local floweret's. The two rectangular features, C, at about 20° to the horizontal are the craters formed by the secondary ion mass spectrometry ion-erosion process used to obtain the depth profiles. The short length of the craters is ~300 μm.

feature of the data in Fig. 7, though, is that H and D both rapidly diffuse into the tetragonal crystal exposed to water. As with the data in Fig. 4, the concentration profiles of H and D are very similar in shape.

Morphologically, the tetragonal crystals were featureless before annealing in water except for surface scratches from the polishing. However, after exposure to water, the surfaces were covered with features that to the eye gave an "orange peel" contrast and by optical microscopy were revealed to be irregular-shaped floweret's. No such features were observed on the surfaces of the cubic crystals after exposure or on the tetragonal crystals annealed in ^{18}O gas. Several of the exposed tetragonal crystals with the "orange peel" appearance were subsequently annealed in air at 1200°C for 2 h, after which the surface features disappeared. This is illustrated in the photomicrographs in Fig. 8. Raman microscopy of the surfaces indicated that the surface features were monoclinic zirconia whereas the surrounding areas were tetragonal, as were the crystals initially. By utilizing the confocal capabilities of the Raman microscope, the transformed regions were found to only extend a short distance into the crystals and when the microscope was focused below the surface no monoclinic phase was detectable (Fig. 9). These Raman microscopy observations are fully consistent with the atomic force microscopy observations made by Chevalier and colleagues of polycrystalline yttria-stabilized zirconia after LTD.[13] Those investigators were able to identify the crystallographic features of the transformed regions and showed them to be fully consistent with the established crystallography of martensite in zirconia. Furthermore, they also showed that the

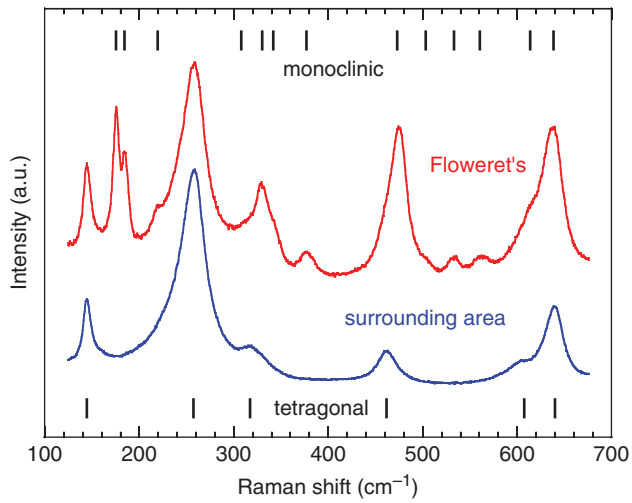

Fig. 9. Raman spectra of the tetragonal crystal before and after immersion. Raman spectra from the floweret's, such as F in Fig. 8, indicate that they are monoclinic regions whereas the surface in between the floweret's is untransformed and has remained tetragonal.

monoclinic regions were almost pyramidal in shape with decreasing cross section with distance into the surface.

IV. Discussion

The observations reported here provide direct evidence that moisture-related species diffuse into tetragonal yttria-stabilized zirconia but not into yttria-stabilized cubic zirconia when exposed to water at temperatures at which LTD of tetragonal zirconia has been reported. Complementary microscopy observations of the tetragonal surfaces exposed to water indicate that the transformation to the monoclinic phase is spatially inhomogeneous and that the transformation proceeds in from the surface. These observations raise several issues that will be discussed in the following, specifically the nature of the diffusing species, why they diffuse in tetragonal zirconia but not in cubic zirconia, and how the observed transformation is related to the possible diffusion mechanisms.

The similarity in shape of the diffusion depth profiles for the H, D, and ^{18}O in tetragonal zirconia, for instance in Fig. 4, suggest that the in-diffusion of these species is coupled because it is highly unlikely that each has the same diffusivity, especially because they have very different atomic masses. One possible explanation for the similarity is that the diffusing species is an $O^{18}D$ (OH) species and that the O^{18} and D ions collected in the SIMS analysis are produced as fragments by the interaction of the ion beam with the sample. Although we initially believed this was the explanation based on our concentration profiles before our calibration experiments, we now consider this to be highly unlikely in view of the measurements on the cubic zirconia crystals implanted with D and H. The profiles from these crystals exhibited an apparent $O^{18}D$ diffusion profile even though they were not implanted with O^{18}. This suggests strongly that the $O^{18}D$ species detected are not diffusing species but rather are formed by interaction of the Cs^+ ion beam with the H and D in the crystal during the SIMS analysis. It would also explain why the mass 20 amu profiles in every SIMS run always scaled with those of the D and the O^{18} profiles. In turn this implies that the oxygen and hydrogen ions are in fact the diffusing species, the oxygen by oxygen vacancy diffusion and the hydrogen by some as-yet unidentified mechanism, but coupled in some manner. The simplest explanation for the coupling is to contemplate that the hydrogen substitutes for an oxygen vacancy site and diffuses by the same oxygen vacancy diffusion mechanism as oxygen diffusion does. The coupling would then be a natural consequence of the same vacancy diffusion mechanism. This would also explain why the diffusivity and activation energy we determine from the ^{18}OD species are the same within experimental

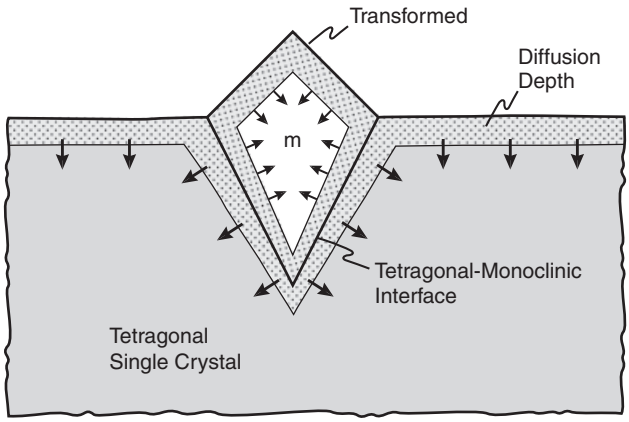

Fig. 10. Schematic illustration of parallel diffusion paths into tetragonal zirconia as moisture-induced transformation to monoclinic occurs at localized regions of the surface.

uncertainty. Alternatively, it is possible that the hydrogen ions could diffuse by an interstitial mechanism, as they do in proton conductors, with coupling through a Coulombic attraction with the oxygen vacancies.[14]

We find that the diffusivity of ^{18}O in cubic and tetragonal crystals exposed to pure ^{18}O gas is consistent with extrapolations of existing ^{18}O in cubic zirconia down to the lower temperatures characteristic of LTD as shown in Fig. 3. We also note that under identical conditions but in water, ^{18}O diffuses into cubic YSZ but that H and D are undetectable above background levels. We are then led to hypothesize that moisture diffusivity in monoclinic is greater than in tetragonal which in turn is larger than in cubic zirconia. Unfortunately, synthetic monoclinic single crystals are unavailable to evaluate. Furthermore, for a direct comparison to be made the monoclinic crystal would have to also contain the same yttria concentration as do the crystals transformed from the tetragonal phase.

The unusual shape of the diffusion profiles shown in Fig. 4 and the observations of the nucleation and growth of the monoclinic regions in the surface of the tetragonal crystal, suggest that during exposure to moisture O and H diffusion occurs along three parallel paths, as illustrated by the schematic in Fig. 10. The first is bulk diffusion through the tetragonal surface which dominates the initial portion of the diffusion profiles. It is from these profiles that our oxygen diffusivities have been determined. Then, as local regions of the surface transform to the monoclinic phase, diffusion can occur along two additional paths; in the monoclinic phase and also along the monoclinic/tetragonal interfaces. If the interfaces were, on average, perpendicular to the surface, then the diffusion profiles would be expected to be similar to the 6/5 dependence characteristic of grain boundary diffusion serving as a parallel path. This would correspond to the well established regime B of diffusion in polycrystalline materials originally described by Hancock and others since.[11] The fact that the interfaces enclose approximately pyramidal (conical)-shaped monoclinic regions and hence are inclined to the surface would not be expected to modify this power law dependence so an alternative explanation is required. (For the same reason, we discount the possibility that the short circuit paths are microcracks rather than monoclinic/tetragonal interfaces). As our data in region B of the profiles in Fig. 4 do not fit a 6/5th dependence on depth, we are therefore led to conclude that the diffusion in region B is dominated by diffusion in the monoclinic phase and the diffusivity is considerably larger in the monoclinic than tetragonal phase. Assuming that the transformed regions are approximately conical in shape, the cross-sectional area of the monoclinic regions decreases linearly with depth below the surface. Then, in region C, the concentration decreases rapidly as only the population of the deepest transformed regions is sampled together with bulk diffusion in the untransformed tetragonal phase deeper in the crystal, ahead of the transformed regions.

The diffusion profiles we record and are illustrated in our figures in this manuscript naturally raise the question as to the possible diffusion mechanism(s). Although it has been suggested that the diffusing species may be a charged oxygen molecule, O_2^-,[8] the majority of papers in the LTD literature assume that the diffusing species is the OH^- ion. The reaction of water with zirconia in terms of OH^- ions as the diffusing species has been formalized in the literature, in the Kroger-Vink notation, as:

$$H_2O + V_O^{\bullet\bullet} + O_O^{\times} \overset{ZrO_2}{\Leftrightarrow} 2(OH)_O^{\bullet} \tag{2}$$

where $(OH)_O^{\bullet}$ is understood to represent an OH^- ion on an oxygen site in the zirconia lattice. The implication is that H and an oxygen ion, which may be loosely bound as a proton circulating an oxygen ion, together diffuse by an oxygen vacancy mechanism. Based on our observations and argued above this seems unlikely. More likely is that H diffuses as a H^+ ion, occupying an oxygen lattice site, and that both O and H diffuse along different physical paths of atomic jumps but by the same oxygen vacancy mechanism. As the diffusion of H and O is driven by the same concentration gradient during exposure to moisture and the diffusion mechanism is the same, then their diffusion appears coupled and it may appear that the diffusing species is an OH^- ion. Thus, it is felt that a more accurate description would be the dissociation of water at the surface of zirconia:

$$H_2O \overset{ZrO_2}{\Leftrightarrow} 2H^+ + O^{2-} \tag{3}$$

followed by the reaction with oxygen vacancy point defects, which in the Kroger-Vink notation

$$2H^+ + O^{2-} + V_O^{\bullet\bullet} \overset{ZrO_2}{\Leftrightarrow} 2H^+ + O_O^{\times} \tag{4}$$

where the reaction would, in turn, be buffered by the stabilizer charge compensation reaction:

$$Y_2O_3 \overset{ZrO_2}{\Leftrightarrow} 2Y'_{Zr} + V_O^{\bullet\bullet} + 3O_O^{\times} \tag{5}$$

In closing this portion of the discussion, we note that the difficulty with LTD mechanisms proposed in the literature that are based on oxygen vacancy diffusion is that one would expect the diffusional fluxes to *increase* with vacancy concentration in the zirconia and, as such, to increase with yttria stabilizer concentration. Thus, it would be expected that H and D would also diffuse into cubic zirconia single crystals since the concentration of oxygen vacancies is even higher in the cubic crystals than in the tetragonal crystals we studied. Clearly, however, as indicated by the results in Fig. 6 neither H nor D diffused into the cubic single crystal after annealing in the isotopically enriched water. There are two possible explanations for this contrary behavior of the hydrogen. The first possibility is that the kinetics of the surface decomposition reaction of water into hydrogen and oxygen are retarded at the surface of the higher yttria content zirconia, perhaps due to changes in surface structure or enhanced surface segregation of Y to the surface sites where the water decomposition occurs. The other possibility is that the higher yttria content alters the energy of the H (and D) in zirconia by altering the Fermi level, namely the electrochemical potential for H depends on the yttria concentration. Experimentally, the absence of any detectable diffusion of H or D into the cubic single crystals when exposed to water is consistent with the reported absence of any LTD of partially stabilized zirconia.[15] This form of stabilized zirconia consists of fine tetragonal spheroidal precipitates embedded in a cubic zirconia matrix. It is also consistent with the fact that yttria-stabilized zirconia used in fuel cells is an anion conductor and not a proton conductor.

Finally, we compare our experimental findings to those in the literature. In fact, the only direct measurement of hydrogen in

zirconia exposed to water that we are aware of is by elastic recoil detection analysis (ERDA).[9] The single measurement presented unequivocally showed that both H and D had diffused into a polycrystalline 3 mol% Y_2O_3 stabilized zirconia ceramic exposed to D-enriched water in an autoclave at 200°C for 2 h. Under the ERDA conditions the authors used, the maximum depth of analysis was 270 nm for D and their analysis indicated that the exposure had led to a concentration of H and D of 1.2×10^{21} atoms/cm^3. Although this concentration must include some contribution from grain boundary diffusion, the majority is likely to be associated with volume diffusion. The ERDA technique is insensitive to the charge state and so cannot provide any information as to the form of the H, whether it is bound as OH^- ions, interstitial H ions or as H_2O molecules. As can be seen in Fig. 4, comparable H concentrations ($\sim 10^{21}$ atoms/cm^3) to those reported from the ERDA measurements[9] are found in region B of the diffusion profiles after 14 h exposure to water at 142°C.

V. Conclusions

Based on SIMS analysis of tetragonal and cubic yttria-stabilized zirconia crystals exposed to isotopically enriched water, and of cubic crystals implanted with H and D, it is concluded that moisture diffusion into zirconia occurs by parallel but independent diffusion of H and O ions. It is also concluded that it is highly unlikely that moisture diffusion occurs by the transport of either water molecules or by the migration of OH ions. The oxygen diffusivity is consistent with extrapolations of oxygen vacancy diffusion in cubic YSZ single crystals to the lower temperatures of moisture-enhanced degradation assuming an activation energy of 1.0 eV. The oxygen diffusivity determined by SIMS analysis of a cubic crystal exposed to ^{18}O gas is the same as that of the same crystal exposed to the isotopically enriched water.

The SIMS analysis also indicates that D and H can diffuse in tetragonal zirconia at room temperature over periods of months. The concentration of H in tetragonal zirconia is similar to that previously reported for a polycrystalline tetragonal zirconia of similar composition exposed under similar conditions. The transformation from tetragonal occurs by the nucleation of small islands of monoclinic phase, evident by their surface relief and Raman spectra, that grow both laterally and into the crystal with time of exposure, consistent with observations made on polycrystalline zirconia. Furthermore, the transformation is reversible and the monoclinic islands transform back to the tetragonal phase and the surface relief associated with the monoclinic islands disappears. It is also surmised that the diffusivity of H and O are faster in yttria-containing monoclinic zirconia than in tetragonal zirconia of the same yttria concentration but confirmation must await availability of single crystals of the monoclinic phase.

Appendix A: SIMS Calibration

To establish calibrations for the sensitivity parameters for H and D in zirconia, a SIMS standard was created by implanting into two cubic yttria-stabilized single crystals. Both H and D were implanted at 33 keV. As with the SIMS data presented in this paper, the calibration profiles were obtained by rastering a 6 keV Cs^+ ion beam across a 300×1000 μm area with an ion current of 250 nA. The secondary ions analyzed came from the center 10% of the rastered area to avoid edge effects and variations in depth. Crater depth was measured using Dektak profilometer. The SIMS depth profiles recorded for the calibration are shown in Fig. 1.

The relative sensitivity factor (RSF) for the implanted ions was calculated with reference to the secondary ion intensity of the Zr, mass 90, by

$$\mathrm{RSF} = C_{\mathrm{ion}} \left(\frac{I_{\mathrm{Zr}}}{I_{\mathrm{ion}}} \right)$$

where C_{ion} is the concentration of the implanted ion in the sputtered volume. The RSF for H and D were calculated to be 1.3×10^{20} and 1.4×10^{20} atoms/cm^3, respectively. It was discovered that the RSF for D could not be reliably used for quantifying the D concentration in the presence of large concentrations of H because the ion beam can create also create pairs of hydrogen atoms by sputtering. These have same mass as D, and consequently cannot be distinguished from D. This difficulty is evident when the background levels of H and D are compared since the natural abundance of D in nature is 1 part of D to 6500 parts H. Nevertheless, it is believed that while this affects the absolute values of the D counts, it does not affect the shapes of the D profiles.

Acknowledgments

The authors are grateful to Dr. Oliver Bierwagen for facilitating the H and D implantations and to Dr. Tom Mates for his advice on the SIMS analysis.

References

[1]K. Kobayashi, H. Kuwajima, and T. Masaki, "Phase Change and Mechanical Properties of ZrO_2–Y_2O_3 Solid Electrolyte After Aging," *Solid State Ionics*, **3/4**, 489–95 (1981).

[2]J. Chevalier, B. Cales, and J. M. Drouin, "Low-Temperature Aging of Y-TZP Ceramics," *J. Am. Ceram. Soc.*, **82** [8] 2150–4 (1999).

[3]J. Chevalier, L. Gremillard, and S. Deville, "Low Temperature Degradation of Zirconia and Implications for Biomedical Implants," *Ann. Rev. Mater. Res.*, **37**, 1–32 (2007).

[4]E. Lilley, "Review of Low Temperature Degradation in Y-TZPs," *Ceram. Trans.*, **10**, 387 (1990).

[5]V. Lughi and D. R. Clarke, "Low-Temperature Transformation Kinetics of Electron-Beam Deposited 5 wt.% Yttria-Stabilized Zirconia," *Acta Mater.*, **55**, 2049–55 (2007).

[6]M. Kilo, C. Argirusis, G. Borchardt, and R. A. Jackson, "Oxygen Diffusion in Yttria-Stabilized Zirconia—Experimental Results and Molecular Dynamics Calculations," *Phys. Chem. Chem. Phys.*, **5**, 2219–24 (2003).

[7]P. S. Manning, J. D. Sirman, R. A. DeSouza, and J. A. Kilner, "The Kinetics of Oxygen Transport in 9.5 mol % Single Crystal Yttria Stabilized Zirconia," *Solid State Ionics*, **100**, 1–10 (1997).

[8]A. E. Hughes, F. T. Ciacchi, and P. S. Badwal, "Role of O^{2-}, OH^- and Anion Vacancies in the Degradation of Y-TZP," *J. Mater. Chem.*, **4** [2] 257–63 (1994).

[9]O. Kruse, H .D. Carstanjen, P .W. Koutouros, H. Schubert, and G. Petzow, "Characterization of H_2O- Aged TZP by Elastic Recoil Detection Analysis"; pp. 163–170 in *Proceedings of the Fifth International Conference on the Science and Technology of Zirconia*, Edited by S. P. S. Badwal, M. J. Bannister, and R. H. J. Hannink. Technomic, Lancaster, PA, 1993.

[10]P. S. Manning, J. D. Sirman, and J. A. Kilner, "Oxygen Self-Diffusion and Surface Exchange Studies of Oxide Electrolytes Having thr Fluorite Structure," *Solid State Ion.*, **93**, 125–32 (1997).

[11]J. Philibert, *Atom Movements, Diffusion and Mass Transport in Solids*. Les Editions de Physique, Les Ulis, France, 1991.

[12]A. D. Le Claire, "The Analysis of Grain Boundary Diffusion Measurements," *Br. J. Appl. Phy.*, **14**, 351–66 (1963).

[13]S. Deville and J. Chevalier, "Martensitic Relief Observation by Atomic Force Microscopy in Yttria-Stabilized Zirconia," *J. Am. Ceram. Soc.*, **86** [12] 2225–7 (2003).

[14]K. D. Kreuer, "Proton Conducting Oxides," *Ann. Rev. Mater. Res.*, **33**, 333–59 (2003).

[15]J. Chevalier, L. Gremillard, A.V. Virkar, and D.R. Clarke, "The Tetragonal–Monoclinic Transformation in Zirconia: Lessons Learnt and Future Trends," *J. Am. Ceram. Soc.* 2009, in Press. □